Magnetic field and temperature dependence of the intrinsic resistance steps in the mixed state of the cuprate superconductor $Nd_{2-x}Ce_xCuO_y$

O. M. Stoll, R. P. Huebener, and S. Kaiser
Physikalisches Institut, Lehrstuhl Experimentalphysik II, Universität Tübingen, Morgenstelle 14, D-72076 Tübingen, Germany

M. Naito
NTT Basic Research Laboratories, 3-1 Morinosato-Wakamiya, Atsugi-shi, Kanagawa, 243-01, Japan
(Received 5 March 1999)

In epitaxial *c*-axis oriented films of the cuprate superconductor $Nd_{2-x}Ce_xCuO_y$ we have studied the magnetic field and temperature dependence of the two intrinsic steps of the flux flow resistance appearing under current bias. The two steps are explained in terms of the field induced energy shift of the normal excitations in the superconducting mixed state. Because of the strong interaction between vortices in the magnetic fields used in our experiments, we propose that narrow subbands develop between the Fermi energy and the energy gap, and that the quasiparticles undergo Bloch oscillations in the subbands, thereby leading to the first resistance step. The second step, appearing at electric fields about a thousand times higher than the fields of the first step, may be explained in terms of a second subband at higher energy or, alternatively, by a sharp upturn of the density of states near the gap energy and of the corresponding phase space available for quasiparticle scattering. [S0163-1829(99)02341-3]

I. INTRODUCTION

Recently, we have reported the observation of an intrinsic step structure of the flux flow resistance in epitaxial *c*-axis oriented films of the cuprate superconductor $Nd_{2-x}Ce_xCuO_y$(NCCO) at intermediate magnetic fields $B_{c1} \ll B < B_{c2}$.[1] NCCO is an electron doped single gap *s*-wave BCS-type superconductor. Our experiments were performed with the samples imbedded in liquid helium, restricting the temperature range to 4.2 K and below. The largest part of our measurements were carried out in superfluid helium, i.e., at $T < 2.17$ K. The details of our experiments can be found in Ref. 1. A typical example of the observed step structure of the voltage-current characteristic (VIC) is shown in Fig. 1 for current bias. Two steps appear in the VIC at the onset voltages V_1 and V_2, respectively. At 1.92 K the voltages V_1 were in the range 10–200 μV, corresponding to the electric-field range $F_1 = (0.3-5) \times 10^{-3}$ V/cm for the typical sample length $L = 360$ μm. The voltages V_2 were about thousand times higher, $V_2 = 200-400$ mV, corresponding to electric fields $F_2 = 5-10$ V/cm.[1] Apparently, the voltage steps at V_1 and V_2 are caused by instabilities due to negative differential resistance. A phenomenological model explaining these instabilities is discussed in Refs. 2 and 3. This model is based on the clean or superclean limit and, specifically, on the energy dependent density of states (DOS) available for quasiparticle scattering. For an isolated vortex the electronic structure of the core is characterized by the energy levels ε_i of the Andreev bound states measured from the Fermi energy ε_F:[4–6]

$$\varepsilon_i = (n + \tfrac{1}{2}) \frac{\Delta^2}{\varepsilon_F} \ln\left(\frac{T_c}{T}\right), \tag{1}$$

where n is an integer and Δ the superconducting energy gap. The enhancement factor $\ln(T_c/T)$ on the right-hand side is due to the Kramer-Pesch effect.[6] An additional sharp upturn of the DOS appears near the superconducting energy gap Δ.[7–9] We emphasize that we restrict our discussion to superconductors with *s*-wave symmetry of the order parameter.

In our previous model considerations[1–3] we have argued that the electric field F generated by vortex motion leads to an energy shift $\varepsilon = eF\nu_F\tau$ of the quasiparticles in the vortex core (e = elementary charge, ν_F = Fermi velocity, τ = electronic scattering time). If this shift reaches energies where a sharp upturn of the DOS and hence of the phase space for quasiparticle scattering appears, we expect a corresponding upturn of the electric resistivity and the onset of negative differential resistivity.[2]

In this paper we report on the magnetic-field dependence and on the temperature dependence of the field values F_1 and F_2 providing further insight into the underlying mechanism. The data on the field F_1 are explained by an extended model

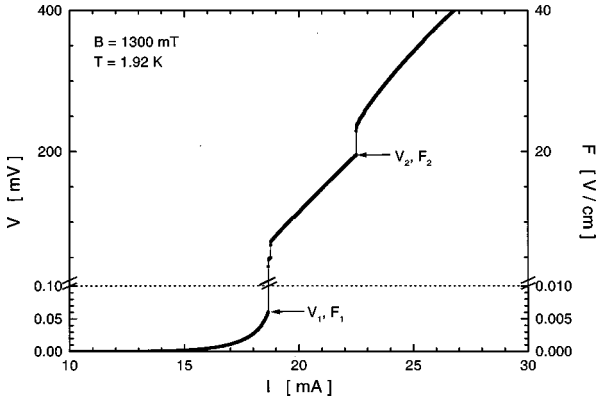

FIG. 1. Typical example of the two voltage steps observed at the onset voltages V_1 and V_2, respectively. The corresponding electric field is indicated on the right vertical axis. Note the change of scale on the voltage axis at $V = 0.10$ mV. $T = 1.92$ K, $B = 1300$ mT.

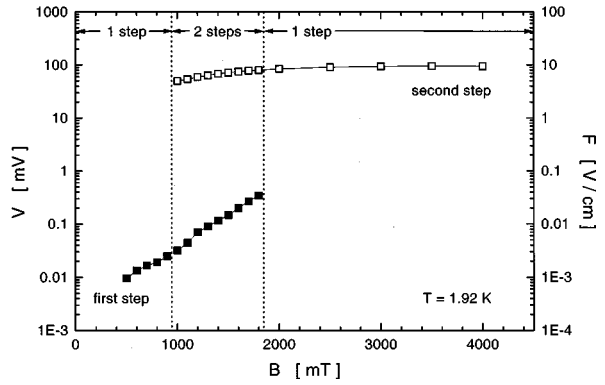

FIG. 2. The onset voltages V_1 (solid squares) and V_2 (open squares) of the first and second voltage steps, respectively, plotted logarithmically versus the magnetic field. The corresponding electric field is indicated on the right vertical axis. $T=1.92$ K.

based on the existence of subbands between the Fermi energy ε_F and the energy gap Δ in the magnetic-field range $B_{c1} \ll B < B_{c2}$. In this way the strong interaction between vortices is taken into account for the clean or superclean limit. Apparently, the negative differential resistivity and the instability at F_1 are caused by Bloch oscillations in the subbands. The instability at the field F_2 is explained in terms of a second subband at higher energy or, alternatively, by the sharp upturn of the DOS near the energy gap providing a strong increase of phase space for quasiparticle scattering.

II. DEPENDENCE OF THE FIRST AND SECOND VOLTAGE STEP UPON MAGNETIC FIELD AND TEMPERATURE

In the course of our experiments we have studied a total of 15 NCCO samples (optimally doped with $x \approx 0.15$ or slightly overdoped with $x \approx 0.16$) all showing similar results. The data shown in the following were obtained for a NCCO film with the following properties: critical temperature $T_c = 21.3$ K; resistivity at 30 K $\rho(30\ \mathrm{K}) = 18\ \mu\Omega$ cm, film thickness $d = 100$ nm; film width $w = 40\ \mu$m. The sample studied carried four voltage leads placed along the bridge with the spacing of 100 μm. The total length between the outer voltage leads was 360 μm.[1] The external magnetic field was applied parallel to the c axis.

In Fig. 2 we present the voltages V_1 and V_2 of the first and second voltage steps, respectively (see Fig. 1), at $T = 1.92$ K as a function of magnetic field B. We see that the appearance of two steps is restricted to the magnetic-field range of about 950–1850 mT. At lower (higher) fields only the lower (higher) step is observed. The voltage V_1 increases nearly exponentially with increasing magnetic field, whereas the voltage V_2 shows a much weaker dependence upon B.

In Fig. 3 the onset voltage V_1 of the lower step is plotted logarithmically versus $(k_B T)^{-1}$ for four different values of the magnetic field (k_B = Boltzmann's constant). The voltage V_1 is seen to increase with increasing temperature, the four curves showing similar behavior. In Fig. 4 the onset voltage V_2 of the upper step is plotted logarithmically versus the temperature for two magnetic fields. In contrast to V_1, the voltage V_2 decreases with increasing temperature.

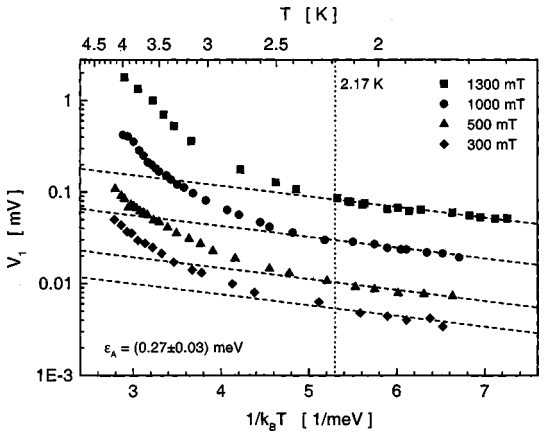

FIG. 3. The onset voltage V_1 of the lower step plotted logarithmically versus $(k_B T)^{-1}$ for four magnetic fields. The dashed straight lines are fitted to the data points taken below 2.17 K.

III. SUBBANDS AND BLOCH OSCILLATIONS IN THE SUPERCLEAN LIMIT

In the clean or superclean limit for an isolated vortex the electronic structure of the core is characterized by the energy levels ε_i of the Andreev bound states measured from the Fermi energy ε_F and given by Eq. (1). For the vortex lattice established in the superconducting mixed state the interaction between vortices must be taken into account. This interaction becomes important if the intervortex distance a becomes equal to or smaller than about the magnetic penetration depth λ. The ratio a/λ is given by

$$\frac{a}{\lambda} = \left(\frac{B_{c1}}{B} \frac{4\pi}{\ln \kappa} \right)^{1/2}, \tag{2}$$

where B_{c1} is the lower critical magnetic field and κ the Ginzburg-Landau parameter. For the intermediate magnetic fields $B_{c1} \ll B < B_{c2}$ of our experiments we have $a < \lambda$ and the vortex interaction is important. In this case the discrete energy levels ε_i of Eq. (1) are expected to broaden into subbands.[10] The width of these subbands increases with decreasing intervortex distance a (increasing B). From this picture we note that the individual vortices loose their prominent electronic identity and are replaced by the subbands between the Fermi energy ε_F and the energy gap Δ. It is

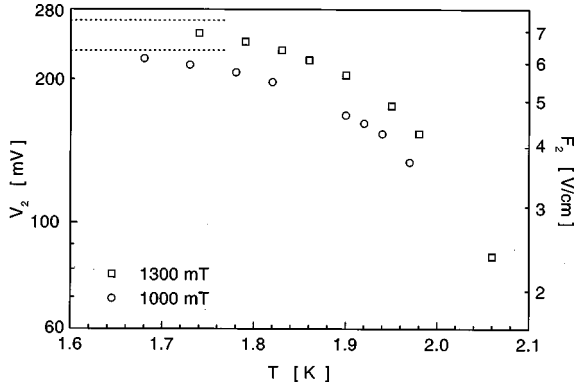

FIG. 4. The onset voltage V_2 of the upper step plotted logarithmically versus the temperature for two magnetic fields. The corresponding electric field is indicated on the right vertical axis.

important to realize that such a scheme must be adopted in the clean or superclean limit, in contrast to the concept of the vortex core of radius ξ with normal-state properties, valid in the dirty limit and exemplified by the Bardeen Stephen model.[11] Because of the quasi-two-dimensional character of the electronic structure in the cuprate superconductors, the DOS near the lower and upper edge of the subbands is nearly energy independent. At $T>0$ the subbands are thermally populated by quasiparticles.

In the presence of the electric field F generated by vortex motion, the particles in the subbands pick up energy and eventually perform Bloch oscillations. (Because of the small energy width of these bands the particles can reach the upper edge of the relevant subband without experiencing a scattering event.) The situation is analogous to the transport of charge carriers in semiconductor superlattices.[12,13] The resistivity is then given by[14,15]

$$\rho=\rho_0(1+\omega_B^2\tau^2)\frac{I_0(\delta\varepsilon/2k_BT)}{I_1(\delta\varepsilon/2k_BT)}, \tag{3}$$

where

$$\omega_B=\frac{eFa}{\hbar} \tag{4}$$

is the Bloch frequency, and $\rho_0=m^*/(ne^2\tau)$. I_0 and I_1 are modified Bessel functions (n=quasiparticle concentration in the subband, τ=electronic scattering time, $\delta\varepsilon$=width of the subband). Equations (3) and (4) yield the proportionality for the current density j:

$$j\sim\frac{F}{1+\left(\frac{F}{F^*}\right)^2} \tag{5}$$

with

$$F^*=\frac{\hbar}{ea\tau}. \tag{6}$$

As a function of the electric field F the current density passes through a maximum at $F=F^*$, and negative differential resistivity sets in at F^*. We propose that the field F_1, at which the first step is observed in the VIC, can be identified with the field F^* given by Eq. (6): $F_1=F^*$. The field F^* and the corresponding Bloch oscillations are associated with the first relevant subband above and below the Fermi energy, respectively. As we see from Fig. 2, between $B=500$ mT and $B=1800$ mT F_1 increases from 1 mV/cm up to 35 mV/cm. Correspondingly, the scattering rate $\tau^{-1}=\omega_B$ increases from $\tau^{-1}=9.6\times10^6\ s^{-1}$ to $\tau^{-1}=177\times10^6\ s^{-1}$, as calculated from $F_1=\hbar/(ea\tau)$.

We emphasize that in our model we concentrate on the quasiparticle dynamics in the subbands and ignore the effects arising from the pair condensate.

IV. DISCUSSION

A. Magnetic-field dependence of F_1 and F_2

As shown in Fig. 2, the field F_1 increases nearly exponentially with increasing B. According to our model the magnetic-field dependence of F_1 results from the proportionality $F_1\sim1/(a\cdot\tau)$, where $1/a\approx(B/\varphi_0)^{1/2}$ contributes the factor $B^{1/2}$. The B dependence of the scattering rate τ^{-1} needs a discussion along the following lines.

In the cuprate superconductors at low temperatures the quasiparticle scattering rate τ^{-1} is dominated by electron-electron scattering.[16–20] Therefore the rate τ^{-1} affecting the field F_1 according to Eq. (6) will depend on the width $\delta\varepsilon$ of the relevant subband, providing the phase space for scattering. Since the exclusion principle must be satisfied twice in electron-electron scattering,[21] we expect

$$\frac{1}{\tau}\sim(\delta\varepsilon)^2. \tag{7}$$

The bandwidth $\delta\varepsilon$ is determined by the overlap between the interacting orbitals and will strongly increase with decreasing intervortex distance (increasing B). In this way the combination of Eqs. (6) and (7) can qualitatively explain the rapid increase of F_1 with increasing magnetic field seen in Fig. 2. Using the approximation $\tau^{-1}=(\delta\varepsilon)^2/\hbar\varepsilon_F$ (Ref. 22) and the value $\varepsilon_F=30$ meV for NCCO,[23] we calculate the values $\delta\varepsilon=0.014$ meV at $B=0.5$ T increasing up to $\delta\varepsilon=0.060$ meV at $B=1.8$ T from the F_1 data of Fig. 2 together with Eq. (6). This appears well consistent with the narrow bandwidth necessary for promoting Bloch oscillations.

Turning next to the field F_2, at which the second step in the resistivity appears, we note that F_2 is about thousand times larger than F_1. We explain this second step of the VIC at the field F_2 in terms of the quasiparticle energy gain at higher electric fields, shifting the distribution function to higher energies. If this shift reaches energies near the gap energy Δ where a sharp upturn of the DOS (Refs. 7–9) and of the associated phase space for quasiparticle scattering occurs, another step in the resistivity is expected. Therefore the field F_2 is approximately given by

$$eF_2v_F\tau=\Delta. \tag{8}$$

Taking for NCCO the values $\Delta=4$ meV (Ref. 24) and $v_F=10^7$ cm/s (Ref. 23) and using the values $F_2=5-10$ V/cm (see Fig. 2), we obtain from Eq. (8) $\tau^{-1}=(1.3-2.5)\times10^{10}\ s^{-1}$. We note that at the higher quasiparticle energies involved in the second resistance step, a quasiclassical energy spectrum can be assumed.

The upturn of the DOS near the energy $\varepsilon=\Delta$ hardly shifts in energy as a function of magnetic field.[7–9] The upturn only becomes less steep with increasing B. This may produce the weak magnetic-field dependence of the threshold field F_2 shown in Fig. 2. Alternately, the second instability at the field F_2 may be explained in terms of another subband at higher energy, in combination with Eq. (6). Again, using the approximation $\tau^{-1}=(\delta\varepsilon)^2/\hbar\varepsilon_F$ we calculate for the bandwidth $\delta\varepsilon=0.51$ meV at 1.0 T increasing up to $\delta\varepsilon=0.69$ meV at 4.0 T.

B. Temperature dependence of F_1 and F_2

It is interesting that the electric onset fields F_1 and F_2 of the lower and upper resistance step respectively, show opposite temperature dependence as seen from Figs. 3 and 4. The quasiparticle scattering rate τ^{-1} affecting the field F_1 ac-

cording to Eq. (6) with $F_1 = F^*$ will be increased because of collisions with particles thermally populating the particular subband. Denoting the relevant activation energy by ε_A, we obtain the proportionality

$$F_1 \sim \tau^{-1} \sim \exp\left(-\frac{\varepsilon_A}{k_B T}\right). \tag{9}$$

The semilogarithmic plot of Fig. 3 indicates that on the low-temperature side the proportionality (9) is reasonably satisfied. In Fig. 3 the dashed straight lines are drawn through the points below the lambda point $T = 2.17$ K. The slope of these straight lines represents the average value $\varepsilon_A = 0.27 \pm 0.03$ meV. It is interesting to compare this value of ε_A with the energy ε_0 of the lowest Andreev bound state in an isolated vortex calculated from Eq. (1). Taking for NCCO the values of Δ and v_F given above, and using $\varepsilon_F = 30$ meV, and $T_c = 21.3$ K, we obtain for $T = 1.9$ K $\varepsilon_0 = \frac{1}{2}(\Delta^2/\varepsilon_F)\ln(T_c/T) = 0.63$ meV. We see that the activation energy ε_A is near 40% of ε_0, which looks reasonable. Since above the lambda point the data in Fig. 3 may be perturbed by Joule heating of the sample, the dashed straight lines in Fig. 3 emphasize the data below $T = 2.17$ K.

From Fig. 3 it appears that the activation energy ε_A is nearly independent of the magnetic field in the range $B = 300-1300$ mT. This confirms that a possible magnetic-field dependence of ε_A is too weak for explaining the strong B dependence of F_1 discussed in Sec. IV A. (This implies that $\delta\varepsilon \ll \varepsilon_A$.)

In contrast to the field F_1, the onset field F_2 decreases with increasing temperature, as we see from Fig. 4. At first sight this looks unexpected. However, in our model the field F_2 may be associated with the field induced quasiparticle energy shift to about the gap energy Δ [see Eq. (8)]. However, at finite temperatures thermal quasiparticle excitation must be taken into account, leading to a reduction of the value of F_2 calculated from Eq. (8). An excellent fit of the experimental values of F_2 is obtained, using a reduction factor of the form $[1-\exp(-\varepsilon_\Delta/k_B T)]$ and writing

$$F_2 = F_0[1-\exp(-\varepsilon_\Delta/k_B T)]. \tag{10}$$

Treating F_0 and ε_Δ as fit parameters, we see in Fig. 5 that an excellent fit of the experimental values of F_2 with Eq. (10) can be obtained. From this fit for the two magnetic fields $B = 1000$ mT and $B = 1300$ mT we obtain the value $\varepsilon_\Delta = 2.20$ meV, i.e., about 55% of the energy gap Δ. The F_0 values found from the fit are $F_0 = 6.38$ V/cm for 1000 mT, and $F_0 = 7.45$ V/cm for 1300 mT. These values of F_0 are marked by the dashed straight lines on the upper left in Fig. 4. The latter considerations can be taken over, if we associate the second instability at the field F_2 with another subband at higher energy.

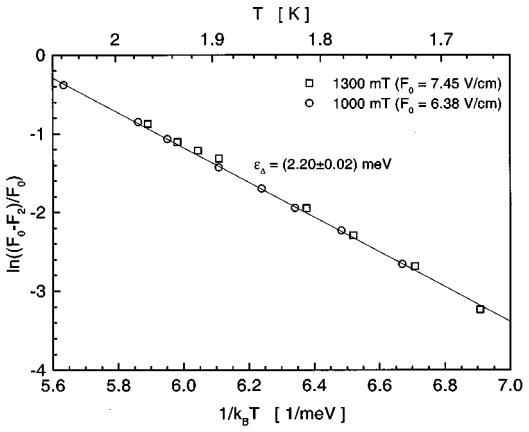

FIG. 5. $\ln[(F_0-F_2)/F_0]$ plotted versus $(k_B T)^{-1}$ for two magnetic fields. The solid straight line represents the fit function given in Eq. (10).

V. SUMMARY AND CONCLUSIONS

In epitaxial *c*-axis oriented films of the optimally doped cuprate superconductor NCCO under current bias two steps in the flux flow resistance have been observed. The observed instabilities provide interesting information on the dynamics of the normal excitations in the superconducting mixed state. In a phenomenological model the two steps can be understood in terms of the field induced energy shift of the quasiparticles. For explaining the magnetic field and temperature dependence of the first step we propose a model based on the appearance of subbands between the Fermi energy and the energy gap. The subbands originate from the discrete energy levels of the Andreev bound states in the core of an isolated vortex in the case where the interaction between vortices becomes important. Because of the small energy width of the subbands in the presence of an electric field the particles in the subbands perform Bloch oscillations, leading to negative differential resistivity.

The electric field at the second step is about a thousand times higher than that at the first step. This second step is explained in terms of the field induced shift of the quasiparticle energy to values near the gap energy, where a sharp upturn of the DOS and of the corresponding phase space available for quasiparticle scattering occurs. In an alternate explanation, the second step is associated with another subband at higher energy. For a satisfactory quantitative understanding, a detailed theoretical analysis is needed.

ACKNOWLEDGMENTS

Financial support of this work by the Deutsche Forschungsgemeinschaft and useful discussions with U. Fischer and N. Schopohl are gratefully acknowledged.

[1] O. M. Stoll, S. Kaiser, R. P. Huebener, and M. Naito, Phys. Rev. Lett. **81**, 2994 (1998).

[2] R. P. Huebener, S. Kaiser, and O. M. Stoll, Europhys. Lett. **44**, 772 (1998).

[3] R. P. Huebener, O. M. Stoll, and S. Kaiser, Phys. Rev. B **59**, R3945 (1999).

[4] C. Caroli, P. G. De Gennes, and J. Matricon, Phys. Lett. **9**, 307 (1964).

[5] J. Bardeen, R. Kümmel, A. E. Jacobs, and L. Tewordt, Phys. Rev. **187**, 556 (1969).

[6] L. Kramer and W. Pesch, Z. Phys. **269**, 59 (1974).
[7] M. Cyrot, Phys. Kondens. Mater. **3**, 374 (1965).
[8] U. Brandt, W. Pesch, and L. Tewordt, Z. Phys. **201**, 209 (1967).
[9] K. Maki, Phys. Rev. **156**, 437 (1967).
[10] E. Canel, Phys. Lett. **16**, 101 (1965).
[11] J. Bardeen and M. J. Stephen, Phys. Rev. A **140**, 1197 (1965).
[12] L. Esaki and R. Tsu, IBM J. Res. Dev. **14**, 61 (1970).
[13] M. Helm, Semicond. Sci. Technol. **10**, 557 (1995).
[14] F. G. Bass and E. A. Rubinshtein, Fiz. Tverd. Tela (Leningrad) **19**, 1379 (1977) [Sov. Phys. Solid State **19**, 800 (1977)].
[15] R. A. Suris and B. S. Shchamkhalova, Sov. Phys. Semicond. **18**, 738 (1984).
[16] A. Virosztek and J. Ruvalds, Phys. Rev. B **42**, 4064 (1990); **45**, 347 (1992).
[17] J. Ruvalds and A. Virosztek, Phys. Rev. B **43**, 5498 (1991).
[18] C. C. Tsuei, A. Gupta, and G. Koren, Physica C **161**, 415 (1989).
[19] D. M. Newns, C. C. Tsuei, P. C. Pattnaik, and C. L. Kane, Comments Condens. Matter Phys. **15**, 273 (1992).
[20] C. T. Rieck, W. A. Little, J. Ruvalds, and A. Virosztek, Phys. Rev. B **51**, 3772 (1995).
[21] J. M. Ziman, *Electrons and Phonons* (Clarendon, Oxford, 1960).
[22] N. W. Ashcroft and N. D. Mermin, *Solid State Physics* (Holt, Rinehart and Winston, New York, 1976).
[23] C. P. Poole, H. A. Parach, and R. J. Creswick, *Superconductivity* (Academic, San Diego, 1995).
[24] S. M. Anlage, D. Wu, J. Mao, X. X. Xi, T. Venkatesan, J. L. Peng, and R. L. Greene, Phys. Rev. B **50**, 523 (1994).